Available online at www.sciencedirect.com
ScienceDirect
Ceramics International 34 (2008) 1121–1125
CERAMICS INTERNATIONAL
www.elsevier.com/locate/ceramint

Raman scattering and electrical conductivity of nitrogen implanted MoO_3 whiskers

S. Phadungdhitidhada *, P. Mangkorntong, S. Choopun, N. Mangkorntong

Department of Physics, Faculty of Science, Chiang Mai University, Chiang Mai 50200, Thailand

Available online 5 October 2007

Abstract

Whiskers of MoO_3 have been grown by a thermal transport process. A set of samples was then implanted with nitrogen ions at a dose of 5×10^{16} ion/cm^2. The implanted whiskers changed from transparent to semi-transparent. Raman spectroscopy of the whiskers was observed and compared with those of unimplanted whiskers. The results revealed that the Raman intensity of the implanted whiskers was decreased about 10 times with respect to that of unimplanted whiskers. Only the case of the wave propagation parallel to the *a*-axis, a lower suppression ratio of the B_{3g} modes was observed. No extra mode due to the nitrogen implantation was observed. This indicates that implantation could only induce defects and oxygen vacancies but not the structural transformation. From electrical conductivity and Hall measurement, it was found that the whiskers exhibited an n-type semiconductor and its conductivity drastically increased due to the defects and oxygen vacancies.

Keywords: Ion implantation; Raman spectroscopy; Thermal transport; MoO_3 whisker

1. Introduction

Molybdenum trioxide (MoO_3) is a layered material which can be used in various types of applications. These include catalysts, photoluminescence, photochromisms, electrochromisms, sensors, and batteries [1]. Due to its optical and electronic properties, MoO_3 has become a promising material for applications in electrochromic systems ranging from microbatteries and gas sensing to devices for information displays [2].

Ion implantation is known as an effective technique to change some physical properties of a material such as electrical property [3]. MoO_3 is a wide band and indirect gap, which is an insulator at room temperature. The implantation of hydrogen ion into MoO_3 pellet to form MoO_3 bronze has been conducted previously [4]. The details of Raman spectra of MoO_3 single crystal and powder have also been realized and reported [5]. The influence of different amounts of oxygen vacancies on the Raman spectra of MoO_{3-x} samples with MoO_3 structure have been studied by Dieterle et al. [6]. They found that I_{283}/I_{290} has a linear relationship with O:Mo ratio. However, the intensity of each Raman peak of the anisotropic crystal structure of MoO_3 is strongly dependent on the orientation of crystal and polarization of the laser source. So far, only the parallel and perpendicular to the *c*-axis have been reported [7].

In this research, the nitrogen implantation of MoO_3 has been performed for the first time and their properties have been studied. The Raman spectroscopy of all possible polarization and orientation of the MoO_3 whiskers have also been carried out and described in this paper.

2. Experimental procedure

In this research, the MoO_3 whiskers were grown by using the vapor transport method. Details regarding to crystal growth technique and identification of the whiskers can be found in [8]. The MoO_3 whisker specimen was prepared by attaching a set of whiskers on to an aluminium plate using silver paste. The dimensions of whiskers were approximately 10 mm in length, 1–2 mm in width and 3–5 μm in thickness, respectively. Nitrogen was induced into the specimen by using the ion implantation technique. The 150-kV ion implantor at Department of Physics, Chiang Mai University [9] was used to perform this process. The nitrogen ions were extracted from the ion source and moved forward directly to the target without using the mass analyzer, so that both N^+ and N_2^+ were in the

* Corresponding author. Tel.: +66 53 943 375; fax: +66 53 357 511.
E-mail address: surelity@gmail.com (S. Phadungdhitidhada).

0272-8842/$34.00
doi:10.1016/j.ceramint.2007.09.093

beam. The nitrogen ions were then implanted into the whiskers with the energy of 60 keV, under the vacuum of 2×10^{-5} mbar and a rough dose of approximately 5×10^{16} ion/cm^2. After the implantation process, it could be observed that the implanted whiskers changed from transparent to semi-transparent. The Raman spectroscopy using the 514.5 nm Ar^+ laser with a backscattering optical configuration was then used in order to investigate and compare the characteristics of the implanted and unimplanted whiskers. The orientation of the implanted whiskers and the laser polarization were taken into account for analysis. The electrical conductivity of the whiskers was measured by using the HP E3633A DC power supply and the HP 34970A multimeter at the temperature ranging from 25 to 200 °C. The Hall measurement was also used to explore the electrical concentration of the implanted whiskers in this research.

3. Results and discussion

3.1. Raman spectroscopy analysis

MoO_3 has an orthorhombic crystal structure consisting of double layers of distorted MoO_6 octahedral held together by covalent forces in the *a* and *c*-axis directions and by the weaker Van der Waals forces in the *b*-axis direction. The Mo–O distance of the distorted octahedrons and three inequivalent oxygen atoms—namely O1, O2, and O3, respectively are shown in Fig. 1. The length of the shortest bond is 1.67 Å. This corresponds to the Mo–O1 bond. In the *a*-axis direction, there are two Mo–O3 bonds with the distances of 2.23 Å and 1.73 Å, respectively. There are three bondings between O2 and Mo. Two equal bondings are along the *c*-axis with the distance of 1.95 Å. The third bonding is in the *b* axis direction with the distance of 2.33 Å. The space group is D_{2h}^{16}. There are 16 atoms in a unit cell. Four atoms are molybdenum and the remainders are oxygen. This results in 48 eigenmodes at the center of Brillouin zone ($q = 0$) which can be described by the displacements of the atoms. This could be either parallel or perpendicular to the chain axis *c*. The irreducible representation is given as:

$$\Gamma = 8A_g + 8B_{1g} + 4B_{2g} + 4B_{3g} + 4A_u + 3B_{1u} + 7B_{2u} + 7B_{3u}$$

where A_g, B_{1g}, B_{2g}, and B_{3g} are Raman-active modes, A_u is an inactive mode, and the remainders are infrared-active modes.

Table 1
Raman selection rules for backscattering corresponding to all possible cases

Cases	Scattering configuration	Allowed modes	Tensor components
$k\|\|a$, $E\|\|b$	$x(yy)\bar{x}$	A_g	α'_{yy}
	$x(yz)\bar{x}$	B_{3g}	α'_{yz}
$k\|\|a$, $E\|\|c$	$x(zz)\bar{x}$	A_g	α'_{zz}
	$x(zy)\bar{x}$	B_{3g}	α'_{yz}
$k\|\|b$, $E\|\|a$	$y(xx)\bar{y}$	A_g	α'_{xx}
	$y(xz)\bar{y}$	B_{2g}	α'_{xz}
$k\|\|b$, $E\|\|c$	$y(zz)\bar{y}$	A_g	α'_{zz}
	$y(zx)\bar{y}$	B_{2g}	α'_{xz}
$k\|\|c$, $E\|\|a$	$z(xx)\bar{z}$	A_g	α'_{xx}
	$z(xy)\bar{z}$	B_{1g}	α'_{xy}
$k\|\|c$, $E\|\|b$	$z(yy)\bar{z}$	A_g	α'_{yy}
	$z(yx)\bar{z}$	B_{1g}	α'_{xy}

The Raman tensors corresponding to A_g, B_{1g}, B_{2g}, and B_{3g} are:

$$\begin{pmatrix} \alpha'_{xx} & 0 & 0 \\ 0 & \alpha'_{yy} & 0 \\ 0 & 0 & \alpha'_{zz} \end{pmatrix}, \begin{pmatrix} 0 & \alpha'_{xy} & 0 \\ \alpha'_{xy} & 0 & 0 \\ 0 & 0 & 0 \end{pmatrix}, \begin{pmatrix} 0 & 0 & \alpha'_{xz} \\ 0 & 0 & 0 \\ \alpha'_{xz} & 0 & 0 \end{pmatrix}$$

and $\begin{pmatrix} 0 & 0 & 0 \\ 0 & 0 & \alpha'_{yz} \\ 0 & \alpha'_{yz} & 0 \end{pmatrix}$,

respectively.

These Raman tensors lead to the selection rules for the six cases of our experiment as given in Table 1.

Fig. 2 shows the Raman spectra of the unimplanted MoO_3 whiskers in the frequency range of 60–1100 cm^{-1}. The intensity of the Raman peaks varies based on the crystal orientation and polarization of the laser source. All the Raman peaks observed are in good agreement with that which has been described in the literature [5]. However, some of the Raman peaks observed in this research will be discussed by apply the selection rules derived from Raman tensors and together with the single crystal MoO_3 reported by Py and Maschke [5].

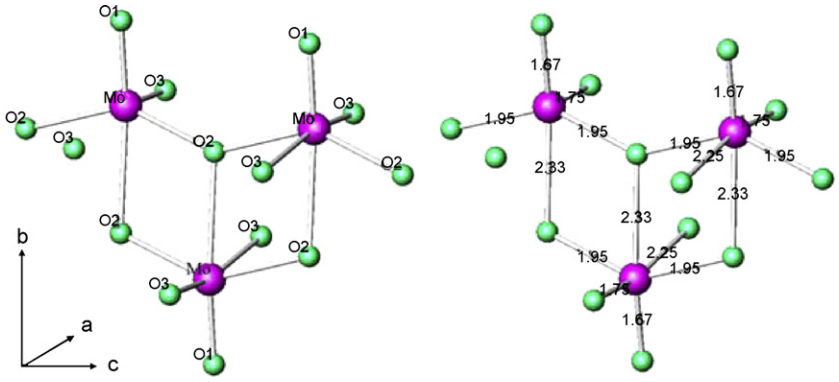

Fig. 1. The crystal structure with labeled atoms and the length of each bond in the crystal structure.

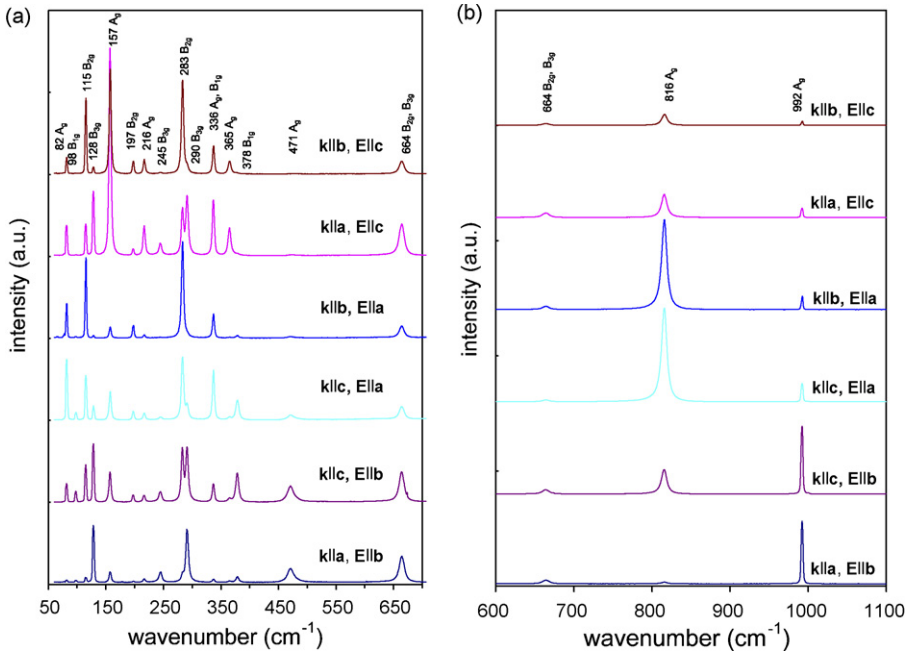

Fig. 2. Raman spectra of unimplanted whiskers taken from six cases of crystal orientation and polarization: (a) 50–700 cm^{-1} and (b) 650–1100 cm^{-1} with the intensity eight times stronger than that in (a).

Three main regions appear for the MoO_3 vibration at 1000–600, 400–200, and below 200 cm^{-1} which correspond respectively to the stretching, deformation, and lattice modes. The Raman peaks at 992 and 816 cm^{-1} are the A_g mode. This corresponds to the ν_{as} Mo = O1 stretching in which the bonding aligns along the *b*-axis direction and the ν_s Mo–O3–Mo stretching in which the bonding aligns along the *a* axis direction, respectively. This results in a drastically change of intensity when polarization occurs in these directions. The peak at 471 cm^{-1} is the A_g mode which corresponds to the ν_{as} M–O2 stretching and bending. This peak appeared only in the case of using polarization aligned along the *b*-axis direction ($E||b$) and should assign to be the stretching of the 2.33 Å Mo–O2 bonding. The peak at 378 cm^{-1} is the B_{1g} mode, corresponding to the δ O2–M–O2 scissor. As seen in Fig. 2a for the cases of $k||c$ & $E||a$ and $k||c$ & $E||b$, its Raman intensity is maximum in the case of the wave propagates parallel with the *c*-axis ($k||c$).

The peak at 365 cm^{-1} is the A_g mode and therefore corresponds to the δO2–M–O2 scissor. Its Raman intensity is maximum in the case of $E||c$, due to the variation of the angle between the two 1.95 Å Mo–O2 bondings lying in the *bc* plane and also corresponds to the selection rule. The peaks at 283 and 290 cm^{-1} are the B_{2g} and B_{3g} modes. This corresponds to the δO1 = M = O1 wagging. The B_{2g} mode intensity should be higher in the case of $k||b$ than that of other cases whereas the B_{3g} mode intensity should be higher in the case of $k||a$.

The peak at 157 cm^{-1} is the A_g mode. This corresponds to the $\delta(O_2Mo_2)_n$ polyhedron along with the chain axis. Its intensity increased strongly when polarizing along the *c*-axis direction. The peaks at 82, 98, 115, and 128 cm^{-1} are the A_g, B_{1g}, B_{2g}, and B_{3g} modes, respectively, corresponding to the translational rigid MoO_4 chain mode. The intensity of the A_g peak was at the maximum when polarizing along the *a*-axis. According to the selection rules, the B_{1g}, B_{2g}, and B_{3g} intensities were at the maximum in the case of $k||c$, $k||b$, and $k||a$, respectively.

Fig. 3a shows examples of the Raman spectra of the implanted MoO_3 whiskers in comparison to that of the unimplanted MoO_3 whiskers. No extra peaks appeared on the entire Raman spectrum of the N^+ implanted whiskers. The

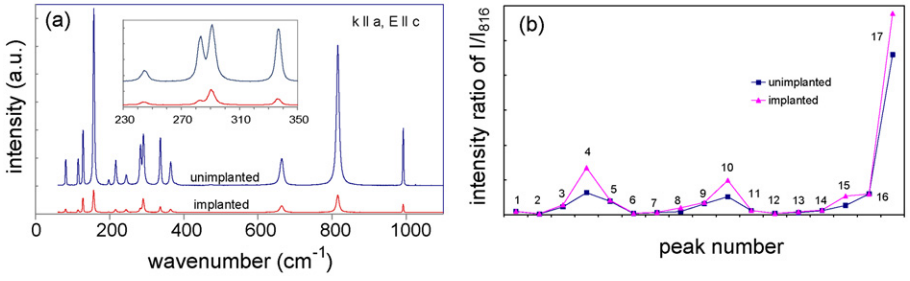

Fig. 3. Raman spectra of implanted and unimplanted whiskers in the case of $k||a$ & $E||c$: (a) 60–1100 cm^{-1} and the inset is an expansion of 230–350 cm^{-1}. (b) The intensity ratio I/I_{816} of the implanted and unimplanted whiskers, where the peaks 1–17 are Raman peaks at 82, 98, 115, . . ., and 992 cm^{-1}, respectively where each peak is the summation of the ratio from all six cases.

intensity of these peaks decreased approximately one order of magnitude with respect to that of the unimplanted whiskers. However, in the case of $k||a$ & $E||c$, the inset in Fig. 3a, the I_{290}/I_{283} ratio of the implanted whiskers was approximately 2.5 times higher than that of the unimplanted whiskers. This was determined by using Gaussian curve fitting. The graph in Fig. 3b shows the relative suppressions of the implanted-Raman peaks of the symmetry modes with respect to the A_g symmetry mode at 816 cm^{-1}. From this graph, it can be seen that most of the A_g, B_{1g}, and B_{2g} modes were suppressed with the same ratio whereas all of the B_{3g} modes (see the peaks 4, 8, 10, and 15 in Fig. 3b) were suppressed with a ratio lower than that of the other modes. Therefore, the B_{3g} modes had a higher ratio of I/I_{816} with respect to the unimplanted ratio, which was derived from the case of $k||a$. No other propagation directions have such an observable difference.

The results of Raman intensity decreasing resemble to that of the H^+ ion implantation on a pellet of MoO_3 with a dose lower than 4×10^{16} ions/cm^2 [4]. This could be explained based on the electronic screening of phonons in the metallic state that the electron transfers from hydrogen to Mo. Therefore, a similar situation could be applied to our results. Dieterle et al. [6] have studied the Raman spectrum of various stoichiometry of MoO_{3-x}. They have found that the ratio of I_{283}/I_{290} decreased linearly as a function of the stoichiometry x, i.e. oxygen vacancy concentration. On the other hand, the distortion due to oxygen vacancy existing in the crystal structure caused the Raman intensity of the B_{3g} mode at 290 cm^{-1} to increase with respect to the B_{2g} mode at 283 cm^{-1}. The comparison between the ratio of I/I_{816} from a single crystal and from polycrystal or film by summing all cases of orientation can be seen in Fig. 3b. This graph suggests that after the implantation, the ratio of I_{283}/I_{290} decreased which was in agreement with what has been observed by Dieterle et al. However, it was worth to summarize that not only the B_{3g} mode at 290 cm^{-1} but all of the B_{3g} modes increased with respect to other modes due to the distortion of the crystal structure from the ion implantation except for the case of $k||a$.

3.2. Electrical properties

In this research, the electrical conductivity (σ) as a function of temperature for the implanted MoO_3 whisker specimens was determined, as shown in Fig. 4. This could be represented by the well known exponential relation:

$$\sigma = A \exp\left(\frac{-E_a}{kT}\right),$$

where A is Arrhenius constants, E_a is the activation energy for the conduction processes, k is the Boltzmann constant and T is the specimen temperature in Kelvin.

From the curve fitting of the data collected from the experiments, the expression above could be written as:

$$\sigma = 3.58 \times 10^{-1} \exp\left(\frac{-0.041\,\text{eV}}{kT}\right) \Omega^{-1}\,\text{cm}^{-1}.$$

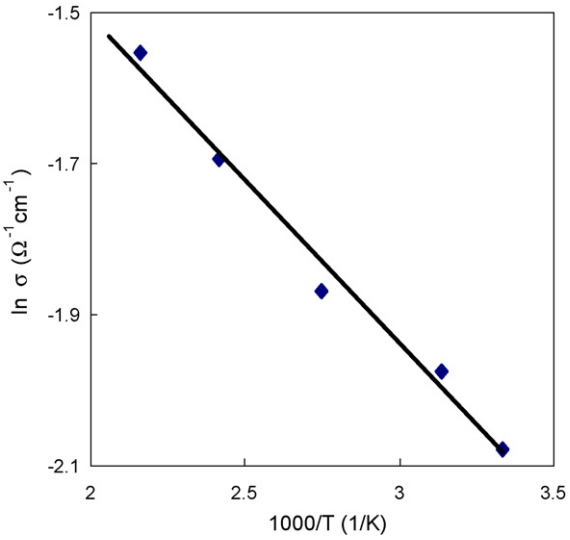

Fig. 4. Electrical conductivity as a function of temperature for the implanted MoO_3 whiskers.

The activation energy of implanted whiskers was about 0.041 eV. The conductivity was enhanced to about 0.074 Ω^{-1} cm^{-1} at a room temperature. This is approximately seven orders of magnitude greater than that of the results from Pandit et al. [10]. From the Hall measurement, the implanted whiskers exhibited as an n-type semiconductor and their electron concentration was about 7×10^{16} cm^{-3}. Pandit et al. reported that MoO_3 exhibits the electrical conductivity differently in two regions of temperature. The higher temperature region was above 380 °C for a single crystal. The activation energy of this region was about 1.75 eV which can be referred to as the intrinsic conduction. For the lower temperature region, the activation energy was about 0.05 eV which was in good agreement with our results. This low activation energy can be categorized as the extrinsic conduction due to impurity, point defects or interstitials, which could not be removed easily [11] and often presented in the forbidden gap of the crystal. From the Raman analysis carried out, it could be confirmed that this is due to the nitrogen ions, which was regarded as impurity, inserted into the layer of the MoO_3 structure and did not bond with Mo. In other words, the implantation of nitrogen ions may increase the electrical conductivity by forming a shallow donor which can be referred to as the n-type conductivity.

4. Conclusions

The Raman spectroscopy of N^+ implanted MoO_3 whiskers was characterized and compared with the unimplanted MoO_3 whiskers in various orientations and polarization directions. The electrical conductivity of the implanted whiskers was also measured. The experimental results have shown that the Raman intensities of the implanted MoO_3 whiskers decrease, with respect to that of the unimplanted whiskers, in which the Raman intensity of the B_{3g} modes were suppressed to a ratio lower than other modes by the distortion due to ion implantation. The distinction of suppression ratio was only in the case of the wave propagation parallel to the a-axis. It

could also be observed that the A_g modes were strongly polarized. Moreover, the electrical conductivity of the MoO_3 whiskers was enhanced obviously by the nitrogen ion implantation and the whiskers exhibited as n-type semiconductor with the activation energy of about 0.041 eV.

Acknowledgements

Surachet Phadungdhitidhada is currently supported by the Grants for Development for New Faculty Staff (GDNFS) Scholarship from the Thai government. We would like to thank the Department of Physics, Faculty of Science, Chiang Mai University, Chiang Mai, Thailand for providing access to its ion implantation facility.

References

[1] C.M. Julien, Lithium intercalated compounds: charge transfer and related properties, Mater. Sci. Eng.: R 40 (2003) 47–102.
[2] K. Bange, Colouration of tungsten oxide films: a model for optically active coatings, Sol. Energy Mater. Sol. Cells 58 (1999) 1–131.
[3] Z. Zhou, K. Kato, T. Komaki, et al., Effects of hydrogen doping through ion implantation on the electrical conductivity of ZnO, Inter. J. Hydrogen Energy 29 (2004) 323–327.
[4] T. Hirata, K. Ishioka, M. Kitajima, Raman spectra of MoO_3 implanted with protons, Appl. Phys. Lett. 68 (4) (1996) 458–460.
[5] M.A. Py, K. Maschke, Intra- and interlayer contributions to the lattice vibrations in MoO_3, Physica B 105 (1981) 370–374.
[6] M. Dieterle, G. Weinberg, G. Mestl, Raman spectroscopy of MoO_3. Part I. Structural characterization of oxygen defects in MoO_{3-x} by DR UV/VIS Raman spectroscopy and X-ray diffraction, Phys. Chem. Chem. Phys. 4 (2002) 812–821.
[7] G.-A. Nazrl, Far-infrared and Raman studies of orthorhombic MoO_3 single crystal, Solid State Ionics 53–56 (1992) 376–382.
[8] S. Choopun, P. Mangkorntong, P. Subjareon, N. Mangkorntong, et al., Orthorhombic MoO_3 whiskers by vapor transport method, Jpn. J. Appl. Phys. 43 (2004) L91–L93.
[9] T. Vilaithong, D. Suwannakachorn, B. Yotsombat, D. Boonyawan, et al., Ion implantation in Thailand (I)—development of ion implantation facilities, ASEAN J. Sci. Technol. Devel. 14 (1997) 87–102.
[10] A.K. Pandit, M. Prasad, T.H. Ansari, R.A. Singh, B.M. Wanklyn, Electrical conduction in MoO_3 single crystal, Solid State Commun. 80 (1991) 125–127.
[11] M.S. Seltzer, R.I. Jaffee, Defect and Transport in Oxides, Plenum Press, New York, 1974, pp. 315–331.